ChemPubSoc Europe

DOI: 10.1002/open.201900146

Open Access ChemistryOPEN Full Papers

Laccase Encapsulation in ZIF-8 Metal-Organic Framework Shows Stability Enhancement and Substrate Selectivity

Tim-Oliver Knedel,[a] Esther Ricklefs,[b] Carsten Schlüsener,[a] Vlada B. Urlacher,[b] and Christoph Janiak*[a]

CgL1 laccase from *Corynebacterium glutamicum* was encapsulated into the metal-organic framework (MOF) ZIF-8 which was synthesized in a rapid enzyme friendly aqueous synthesis, the fastest in situ encapsulation of laccases reported to date. The obtained enzyme/MOF, i.e. laccase@ZIF-8 composite showed enhanced thermal (up to 70 °C) and chemical (N,N-dimethylformamide) stability, resulting in a stable heterogenous catalyst, suitable for high temperature reactions in organic solvents. Furthermore, the defined structure of ZIF-8 produced a size selective substrate specificity, so that substrates larger than the pore size were not accepted. Thereby, 2'-azino-bis(3-ethylbenzothiazoline-6-sulphonic acid) (ABTS) was used to verify that the enzyme is immobilized inside the MOF versus the outside surface. The enzyme@MOF composite was analyzed by atomic absorption spectroscopy (ASS) to precisely determine the enzyme loading to 2.1 wt%.

1. Introduction

Enzyme catalysis has been exploited in industrial processes, such as the synthesis of flavors, pharmaceutical ingredients and fine chemicals.[1] Compared to chemical catalysts, enzymes are regio-, stereo- and chemo-selective.[2,3] Moreover, they catalyze numerous reactions with high turnover rates.[4,5] However, biocatalytic processes often suffers from the poor robustness of enzymes.[6] One option to enhance enzyme stability is their encapsulation in porous materials.[7] Recently, metal-organic frameworks (MOFs) have been suggested as alternative carriers for enzyme immobilization.[8,9] Due to the wide spectrum of organic linkers with varying size and structure the properties and architecture of MOFs can easily be controlled and thereby provide perfect carrier materials for various enzymes.[10] The encapsulation should result in enzyme@MOF composites with size dependent substrate specificity, improved thermal and process stability and prolonged retention of catalytic ability.[11–15] Additionally, enzyme@MOF materials can easily be retrieved by centrifugation or filtration and are thereby usable as heterogeneous catalysts, preventing protein contamination of the samples.[16]

Enzymes, although providing highly regio-, stereo- and chemo-selective catalytic reactions, can still accept a wide spectrum of possible substrates.[17,18] Therefore enhancing the substrate specificity is a desirable property.[19,20] By providing an ordered network of defined pore and canal sizes, MOFs may present an excellent carrier for size selection of substrates.

Enhanced stability is one of the major properties achieved by encapsulation. Biocatalytic processes often involve organic solvents as reactant or product and require temperatures higher than room temperature. Thus, solvent and thermal stability is one of the most important properties for enzymes.[21,22] Beside the thermal and chemical stability, a biocatalyst must be well separable without great effort. Moreover, one of the disadvantages of many immobilized enzymes is their leaching during reaction in solution.[23] *Falcaro* et al. have shown that thermal stability of urease could be enhanced by encapsulation in ZIF-8. They were able to encapsulate 15% of the deployed free enzyme, resulting in a composite that retained nearly 40% remaining enzymatic activity after 30 min incubation at 80 °C. By comparison, the free enzyme could barely keep any activity under these conditions.[7] In addition, the encapsulation of horseradish peroxidase (HRP) in ZIF-8 resulted in a significant higher stability of the enzyme against boiling solvents. In both, boiling water and boiling DMF, nearly 90% of the substrate was converted, whereas the unprotected enzyme completely lost its activity.[24] Encapsulation in MOFs can also be used for the co-immobilization of several enzymes. *Wu* et al. could create multiple enzyme-embedded MOFs by encapsulating glucose oxidase and horseradish peroxidase in ZIF-8, which resulted in a composite with enhanced thermal stability.[25] This composite retained more than 80% of its activity after 7 days, whereas free enzymes only kept around 50% of their activity. *Lyu* et al. showed, that enzyme encapsulation in MOFs can not only enhance thermal stability, but also enzyme activity. They embedded cytochrome c in ZIF-8, resulting in a composite with a 10-fold higher activity compared to the free enzyme.[26]

[a] *T.-O. Knedel, C. Schlüsener, Prof. Dr. C. Janiak*
Institut für Anorganische Chemie und Strukturchemie,
Heinrich-Heine-Universität Düsseldorf
40204 Düsseldorf
E-mail: janiak@uni-duesseldorf.de
[b] *Dr. E. Ricklefs, Prof. Dr. V. B. Urlacher*
Institut für Biochemie
Heinrich-Heine-Universität Düsseldorf
40204 Düsseldorf

Supporting information for this article is available on the WWW under https://doi.org/10.1002/open.201900146

© 2019 The Authors. Published by Wiley-VCH Verlag GmbH & Co. KGaA. This is an open access article under the terms of the Creative Commons Attribution Non-Commercial NoDerivs License, which permits use and distribution in any medium, provided the original work is properly cited, the use is non-commercial and no modifications or adaptations are made.

Laccases (EC 1.10.3.2) belong to the group of multicopper oxidases.[27] They contain four copper ions, which are responsible for the catalytic activity.[28,29] Laccases are widespread in nature and found in plants, fungi, insects, yeast and bacteria.[30–32] Laccases catalyze oxidation of a broad range of substrates, including mono-, di- and polyphenols, aromatic and aliphatic amines, benzenethiols as well as organic and inorganic metal compounds coupled to the four electron reduction of molecular oxygen to water.[17]

Due to their broad substrate scope and ability to produce water as the only coproduct laccases are considered potential biocatalysts for industrial processes in the food and textile industry, synthetic chemistry and bioremediation.[33] Their application is, however, inhibited by chelating agents like azides, high halide anion and metal cation concentrations as well as some organic solvents.[34,35] Significant efforts have been undertaken to stabilize laccases and protect them from inhibiting agents by immobilization via adsorption, covalent binding and encapsulation.[36,37] Recently, nanocrystalline MOFs were used for the immobilization of laccases. Thereby, in the most successful cases post-synthesis immobilization (PSI) was applied.[38,39,40,41] An exception to PSI was the work by *Patil* et al. and *Naseri* et al., presenting a novel method for the *in situ* encapsulation of laccases in ZIF-8.[42,43]

Here we demonstrate the *in situ* encapsulation of the CgL1 laccase from *Corynebacterium glutamicum* in ZIF-8. Different to the previously used MOFs for post-synthetic immobilization, the pores and windows (aperture diameter 3.4 Å) of ZIF-8 are too small for laccases, making it impossible to immobilize the enzyme by PSI.[44] Nevertheless ZIF-8 is very well suited for immobilizing enzymes, because it can be synthesized under enzyme-friendly conditions with water as a solvent, at room temperature and during a short reaction time.[45] Different to the work of *Patil* et al. and *Naseri* et al., the reaction time was cut from 20 min and 12 h, respectively, to only 5 min in our work.[42,43] Therefore, we provide the fastest *in situ* encapsulation of laccase in ZIF-8 to this day, resulting in a composite with enhanced solvent and temperature stability and novel size selective specificity against large substrates.

2. Results and Discussion

For laccase@ZIF-8 preparation, a portion of 250 µL laccase solution (15 mg/mL) in potassium phosphate buffer, pH 7.5, was added to a solution of 2-methylimidazole in purified water. Then zinc nitrate hexahydrate in water were added to the mixture, which was stirred for 5 min at 500 rpm. The resulting suspension was centrifuged for 10 minutes at 10000 rpm and the solid residue was washed two times with 10 mL of purified water. The resulting solid composite was dried overnight at 40 °C and gave a reproducible yield of 100 ± 10 mg of enzyme@MOF composite.

Laccases contain copper ions, whose quantification by atomic absorption spectroscopy (AAS) was used as a first proof for the successful *in situ* laccase encapsulation in ZIF-8. As shown in Table S1, the AAS measurements of free purified laccase gave a copper content of 1.9 ± 0.1 wt%. The measurements of laccase@ZIF-8 yielded 0.040 ± 0.002 wt% Cu (corrected for the copper blind value of ZIF-8). This implies a laccase content of 2.1 wt% in the laccase@ZIF-8 composite or that 55 % of the offered laccase was encapsulated in the MOF. Cross check of the solvent solutions which were retrieved after the encapsulation procedure gave a copper content of 30 ± 3 µg, meaning that 43 % of the used laccase where not encapsulated (Table S1).

The activity of the free and encapsulated laccase was evaluated using 2,6-dimethoxyphenol (2,6-DMP) as substrate (Scheme 1 and S1). Remarkably, on average, laccase@ZIF-8

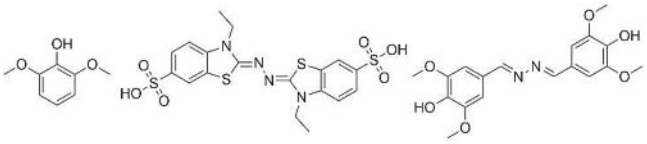

Scheme 1. Structure of the three used substrates 2,6-dimethoxyphenol (2,6-DMP) (left), 2,2′-azino-bis(3-ethylbenzothiazoline-6-sulphonic acid) (ABTS) (middle) and syringaldazine (SGZ) (right).

showed an activity of 4 ± 1 mU, which corresponds to about 7 % of the activity of a 15 mg/mL laccase solution (61 ± 5 mU). Considering the laccase immobilization efficiency of 55 % which was determined by atomic absorption spectroscopy, only 13 % of the encapsulated laccase was active towards 2,6-DMP. This means that either most of the laccase was deactivated during the *in situ* encapsulation, or the substrate 2,6-DMP cannot access the encapsulated laccase inside the MOF particles. Experiments with 2,2′-azino-bis(3-ethylbenzothiazoline-6-sulphonic acid) (ABTS) (Scheme 1), a substrate much larger than 2,6-DMP, showed no activity at all. Since ABTS with its dimensions of 9 by 18 Å is clearly too bulky to enter the pore windows of 3.4 Å diameter of ZIF-8 (even assuming some flexibility and pore widening[46]), this is a good indication that the enzyme is encapsulated inside the MOF and not only immobilized on the surface.

The powder X-ray diffractogram (PXRD) of laccase@ZIF-8 matches the experimental and simulated diffractogram of ZIF-8 (Figure 1). The encapsulation of the enzyme has little effect on the crystallinity of ZIF-8 but the PXRD by itself is no verification of enzyme encapsulation.

The scanning electron microscopy (SEM) image of laccase@ZIF-8 (Figure 2, top) shows spherical ZIF-8 particles of approximately 115 nm ± 20 nm (see histogram Figure 3). The neat ZIF-8 particles (Figure 2, bottom) are slightly smaller, with 105 ± 16 nm (see histogram Figure 3) but the sizes are still within the same range, when considering the one-sigma standard deviation values of ± 20 and ± 16 nm. Due to the fast preparation method no well-shaped ZIF-8 crystals were obtained. As already concluded from PXRD, the encapsulation of the enzyme seems to have no effect on the shape of the MOF particles and due to its small size, laccase cannot be recognized by SEM at this resolution. Also, the copper concentration in the particles is too

© 2019 The Authors. Published by Wiley-VCH Verlag GmbH & Co. KGaA

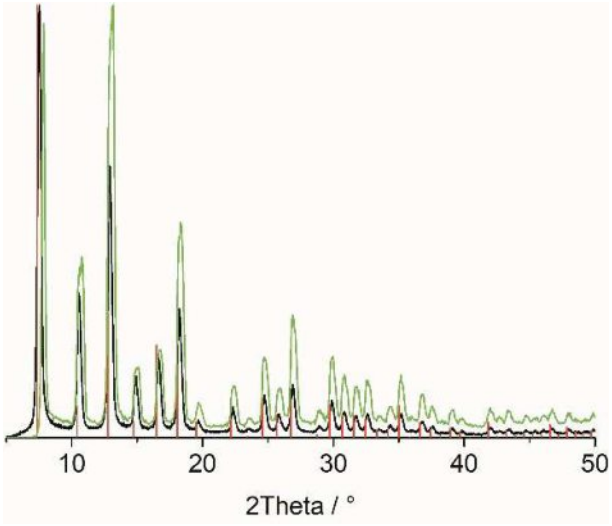

Figure 1. Powder X-ray diffractograms (PXRD) of laccase@ZIF-8 (green), pure ZIF-8 (black) and simulated ZIF-8 (red).

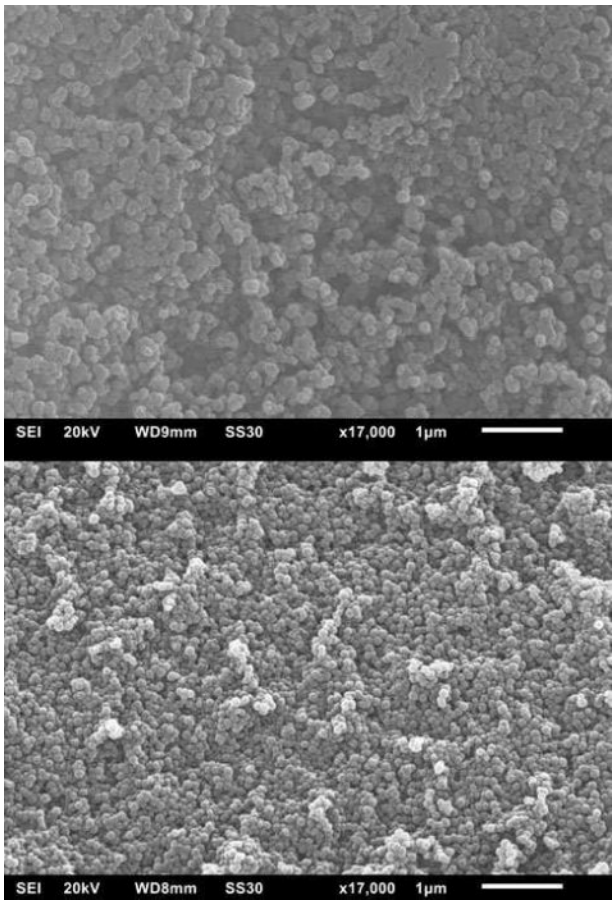

Figure 2. Scanning electron microscopy (SEM) images of laccase@ZIF-8 (top) and neat ZIF-8 (bottom).

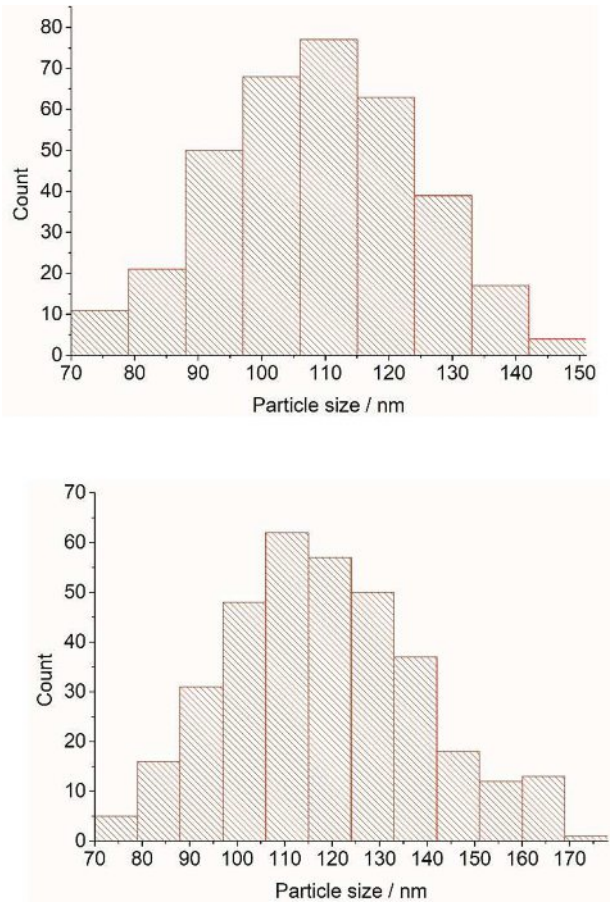

Figure 3. Particle size distribution of 115 ± 20 nm for laccase@ZIF-8 (top) and of 105 ± 16 nm for ZIF-8 (bottom) particles based on evaluation of the SEM images.

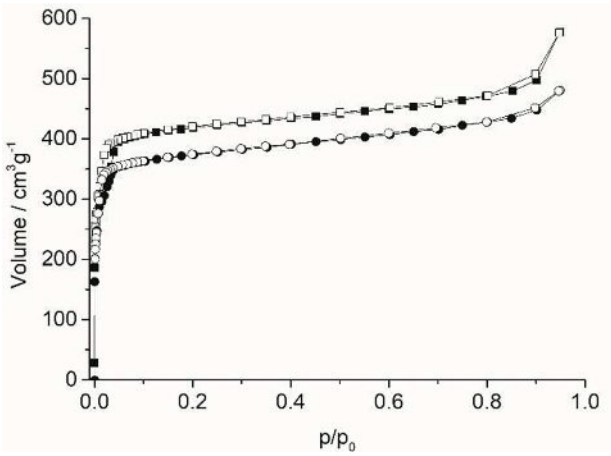

Figure 4. N_2-sorption isotherms of laccase@ZIF-8 (circles) and of neat ZIF-8 (squares). Filled symbols: adsorption, open symbols: desorption.

low to be detected by energy-dispersive X-ray spectroscopy (EDX).

For porosity determination N_2- and Ar-sorption measurements where performed at 77 K and 87 K respectively (Figure 4 and Figure S1). The N_2-sorption isotherms show an approximate Type I shape which is typical for microporous materials and yield a BET-surface-area of 1536 $m^2 g^{-1}$ and a total pore volume of 0.817 $cm^3 g^{-1}$ for neat ZIF-8, in good agreement with the literature surface-areas of 1000 to 1600 $m^2 g^{-1}$ and pore

© 2019 The Authors. Published by Wiley-VCH Verlag GmbH & Co. KGaA

volumes of 0.3 to 1.3 $cm^3 g^{-1}$.[44,47,48,49,50,51] For laccase@ZIF-8 a BET-surface area of 1387 $m^2 g^{-1}$ and a total pore volume of 0.687 $cm^3 g^{-1}$ was obtained, meaning that the encapsulation of laccase in ZIF-8 results in a slightly lower surface-area and pore volume when compared to the synthesis without laccase under otherwise unchanged conditions. Compared to other works, a reduction of the surface area when encapsulating a substrate into ZIF-8 is a result to be expected.[52,53] The reduction of the total pore volume is also expected due to the enzyme likely blocking some of the pores. The micropore volume was calculated from the V–t-plot according to DeBoer to 0.568 $cm^3 g^{-1}$ with a micropore surface area of 1355 $m^2 \cdot g^{-1}$ for ZIF-8 and to 0.490 $cm^3 g^{-1}$ with a micropore surface area of 1186 $m^2 g^{-1}$ for laccase@ZIF-8. The lower total pore volume and micropore volume for laccase@ZIF-8 compared to pure ZIF-8 both indicate, that the enzyme is encapsulated in the pores of ZIF-8.

Substrate specificity of laccase@ZIF-8 was tested using 2,6-DMP, syringaldazine (SGZ, Scheme 1) and ABTS as substrate with free laccase and the composite (Table 1).

Table 1. Activity of encapsulated and free laccase against 2,6-DMP, SGZ and ABTS.

Substrate	Activity laccase [mU]	Activity laccase@ZIF-8 [mU]	Relative activity [%][a]
2,6-DMP	32 ± 2	2 ± 0.1	5 ± 0.1
SGZ	30 ± 1	3 ± 0.4	11 ± 1
ABTS	116 ± 2	0 ± 0.1	0 ± 0.1

[a] Relative activity: (Activity laccase@ZIF-8):(Activity laccase) × 100 %.

The free laccase was able to convert all substrates. The relative activity of 5 % of laccase@ZIF-8 against 2,6-DMP is comparable with the results mentioned before. Although SGZ is considerably larger than 2,6-DMP (approximately 4 × 14 and 4 × 5 Å respectively), laccase@ZIF-8 can convert SGZ, resulting in a relative activity of 10 %. Against ABTS the composite shows no activity at all. Considering the pore window size of ZIF-8 (3.4 Å diameter), SGZ marks the limiting size above which a substrate is not able to enter the pores and being converted by the encapsulated laccase.

To evaluate a possible leaching, laccase@ZIF-8 was incubated for a set time in the reaction mixture and then separated by centrifugation. The remaining 2 mL reaction solution was continued to be measured with the activity assay. The average activity of laccase@ZIF-8 samples before separation was 3.3 ± 0.4 mU. After separation, the activity in the filtrate increased to 5.9 ± 0.7 mU. Additionally, AAS measurements of the filtrate showed that about 20 % of the laccase from laccase@ZIF-8 had leached into the reaction mixture (Table S2). This indicates that the encapsulated laccase features a significantly lower activity due to diffusion-controlled access, but the activity of the free laccase is recovered upon leaching.

We determined the stability of laccase@ZIF-8 in the two solvents ethanol and N,N-dimethylformamide (DMF) in comparison to the stability of free laccase which was assessed under the same conditions (Figure 5).

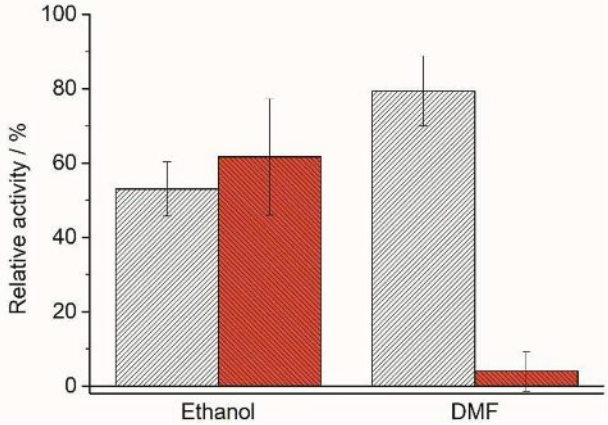

Figure 5. Residual activity towards 2,6-DMP in KPi-buffer of immobilized (white) and free laccase (red) after incubation for 1 h in DMF and ethanol followed by separation (for laccase@ZIF-8) and activity testing. Relative activity: The activity of immobilized and free laccase, respectively, in KPi-buffer before incubation was set to 100 %. Hence relative activity = (Activity in solvent):(Activity in KPi-buffer) × 100 %. The absolute activities are given in Table S4 in the Supp. Info.

After incubation in ethanol or DMF and separation by centrifugation laccase@ZIF-8 retained between 50 % (in ethanol) and 80 % (in DMF) of its initial activity towards 2,6-DMP. A possible explanation for the different relative activities could be the size of the solvents. DMF is a larger molecule compared to ethanol. Therefore, ethanol molecules can enter the pores of ZIF-8 and reach the encapsulated enzyme, resulting in damaging the laccase. Stabilities of the free and encapsulated laccases in ethanol are comparable, which supports this explanation. Compared to the free enzyme, laccase@ZIF-8 shows much higher stability in DMF. Free laccase lost almost all its activity towards 2,6-DMP, whereas the composite retained about 80 % of the initial activity.

For temperature stability determination the enzyme activity was measured after incubation of laccase@ZIF-8 (Figure 6, top) and free laccase (Figure 6, bottom) at different temperatures for up to 6 hours. The results demonstrate that after one hour of incubation, the laccase loses nearly no activity at room temperature. The laccase@ZIF-8 samples at 40 and 60 °C show a loss of activity of 40 and 20 % respectively. The 70 °C sample shows also no loss of activity, but with a very high uncertainty, indicating that the sample probably lost at least a bit of activity compared to the 25 °C reference. After 4 h and 6 h incubation nearly all samples lost around 40 % activity. But compared to the free laccase this is a massive stability enhancement especially for higher temperatures of 60 and 70 °C (Figure 2) Free laccase shows no activity at all after only 3 h at 70 °C and only about 10 % activity at 60 °C. The increase in activity for laccase@ZIF-8 after incubation for 6 h is explained by the disaggregation of the ZIF-8 aggregates which sets the smaller primary particles free. During the incubation of laccase@ZIF-8 for 6 h the larger MOF particle aggregates, consisting of multiple primary 115 nm crystallites (Figure 2), may disaggre-

© 2019 The Authors. Published by Wiley-VCH Verlag GmbH & Co. KGaA

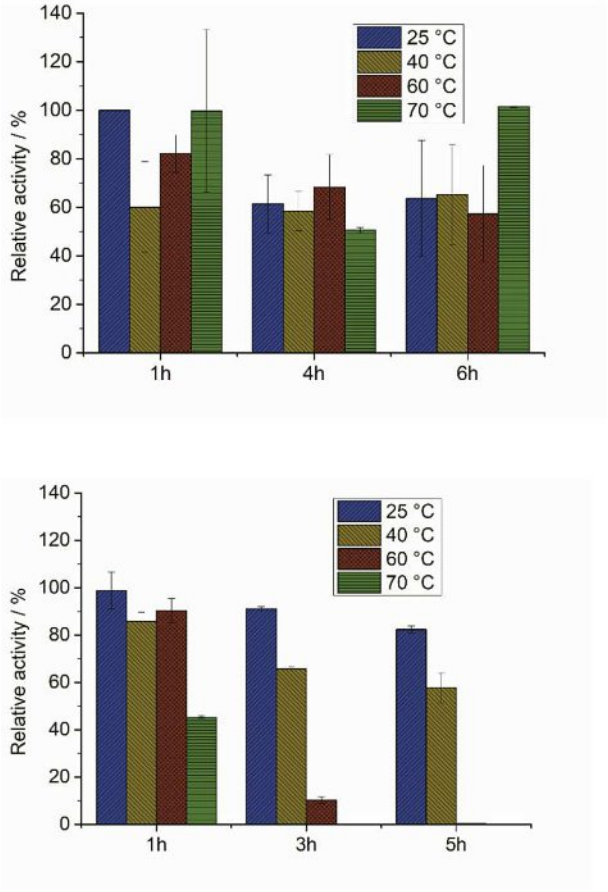

Figure 6. Residual activity towards 2,6-DMP in KPi-buffer of immobilized laccase (top) after incubation for 1 h, 4 h and 6 h and free laccase (bottom) for 1 h, 3 h and 5 h at 25 °C, 40 °C, 60 °C and 70 °C in potassium phosphate buffer. Relative activity: The activity after 1 h incubation at 25 °C was set to 100 % as reference; hence relative activity = (Activity at given temperature, T and incubation time, t):(Activity at T = 25 °C, t = 1 h). The absolute activities are given in Table S5 in the Supp. Info. Results for free laccase were adapted from ref. 17. See the note in the Experimental Section on the large error bars in Figure 6 top.

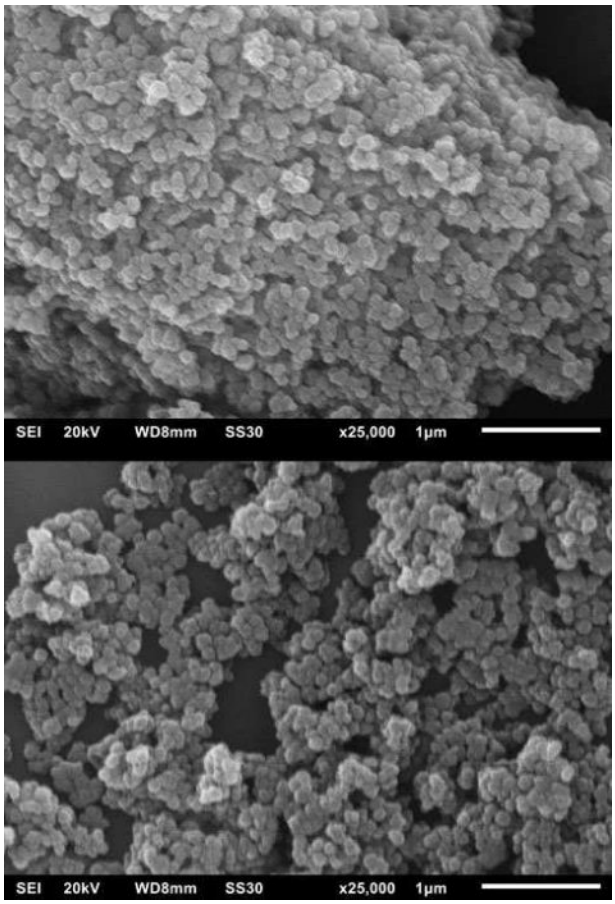

Figure 7. Scanning electron microscopy (SEM) images of laccase@ZIF-8 after 1 h in water 25 °C (top) and after 6 h in water at 70 °C (bottom).

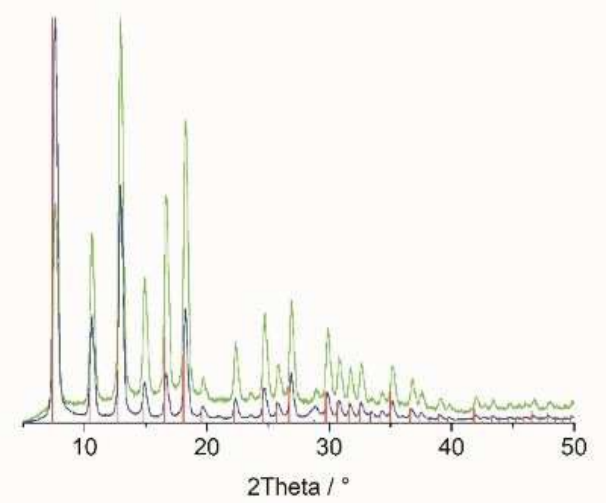

Figure 8. Powder X-ray diffractograms (PXRDs) of laccase@ZIF-8 (green), laccase@ZIF-8 after 6 h at 70 °C (blue) and simulated ZIF-8 (red).

gate to the primary crystallites, resulting in a higher accessible surface area. This would mean that some laccase molecules, that were inaccessible in the beginning, could now be reached by the substrate molecules, yielding a higher activity.

To ensure that the enhanced activity is not a result of concomitant decomposition of the MOF itself, SEM images and PXRD measurements were compared for the sample which was left for 1 h at 25 °C and which had been incubated for 6 h at 70 °C (Figure 7 and Figure 8).

The size and shape of the primary particles remained unchanged, indicating that no decomposition, but some disaggregation had occurred. PXRD measurements of laccase@-ZIF-8 without treatment and after 6 h at 70 °C also indicate that the ZIF-8 remained unchanged (Figure 8). For comparison SEM images were taken also of neat ZIF-8 under the same conditions where again some disaggregation became apparent (see Figure S27).

3. Conclusions

In conclusion, this work describes an easy and fast way to immobilize laccase. With the modified synthesis of ZIF-8 an

© 2019 The Authors. Published by Wiley-VCH Verlag GmbH & Co. KGaA

enzyme-friendly reaction environment was created where nearly 60% of the used enzyme could be encapsulated within only 5 min of reaction time. The received product showed better stability against solvents and temperature than the free enzyme, meaning that the ZIF-8-shell works as a protection against environmental influences. Additionally, the laccase@ZIF-8 is insoluble in organic solvents resulting in a potential application of the product as heterogenous catalyst. Due to the defined pore size of ZIF-8 the composite shows size selective substrate specificity, only accepting substrates smaller than the pore diameter of ZIF-8.

Experimental Section

All reagents were used as purchased. 2-Methylimidazole was obtained from Acros, zinc nitrate hexahydrate and dipotassium hydrogen phosphate from Carl-Roth, 2,6-dimethoxyphenol (2,6-DMP) from Sigma-Aldrich, syringaldazine from SAFC Pharma, ABTS from Sigma-Aldrich, potassium dihydrogen phosphate from Fisher Scientific. Purified water was derived from a Synergy® water preparation system with SynergyPak® processing cartridge from Merck Millipore, with a conductivity of 0.05 µS/cm at 25 °C, and from a GenPure ultrapure water system with UV-photooxidation and ultrafiltration module from TKA, with a conductivity of 0.05 µS/cm at 25 °C.

Enzymes for cloning were obtained from Thermo Fisher Sientific. *E. coli* strain DH5α (F- supE44 ΔlacU169 (ϕ80lacZΔM15) hsdR17 recA1 endA1 gyrA96 thi-1relA1) was purchased from Clontech (Saint-Germain-en-Laye, France), *E. coli* strain BL21 (DE3) (F- ompT hsdSB (rB- mB-) gal dcm (DE3)) and the pET-16b vector from Novagen (Madison, USA).

Atomic absorption spectroscopy (AAS) was carried out on an AAnalyst 100 from Perkin-Elmer with a one element copper hollow cathode in an acetylene/air-flame. Powder X-Ray diffraction (PXRD) patterns were obtained on a Bruker D2 phaser (300 W, 30 kV, 10 mA) using Cu-Kα radiation (λ = 1.54 Å) at ambient temperature with a scanning rate of 0.0125 °/s. The diffractograms were collected with a flat, low-background sample holder, on which the beam spot is strongly broadened at low angle so that only a fraction of the reflected radiation reaches the detector, so that intensities measured at $2\Theta < 7$ have low intensity. SEM images were obtained on a Joel JSM 6510 electron microscope with a LaB_6-cathode at 5–20 keV. Samples for SEM images were prepared on a 120 µm carbon-coated copper grid, by dripping a composite/water suspension onto the grid and removing the solvent from below by placing the grid on a soft tissue. Nitrogen physisorption isotherms were measured on a Nova 4200e S/N from Quantachrome at 77 K. Before the gas sorption experiment, the sample was placed into a pre-weighted glass tube capped with a septum. The tube was connected to the degassing port of the sorption analyzer, degassed under dynamic vacuum of $1 \cdot 10^{-2}$ mbar at 130 °C for 3 h, weighed again and then transferred to the analysis port of the sorption analyzer. The Brunauer-Emmett-Teller, BET surface areas were calculated from the nitrogen adsorption isotherms in the p/p_0 range from 0.017 to 0.07. Total pore volumes were calculated from the nitrogen sorption isotherm at $p/p_0 = 0.95$. DFT calculations for the pore size distribution curves were done with the native 'NovaWin 11.03' software using the 'N_2 at 77 K on carbon, slit pore, NLDFT equilibrium' model. UV/Vis absorption curves were obtained from a GE Healthcare Ultrospec 7000 with 8-fold sample changer (activity of laccase and laccase@ZIF-8) and from a Tecan infinite M200pro with 96 and 384-well-microtiterplate reader for absorption- and fluorescence spectrometrics including an injection system. The measurements were carried out at a wavelength of 468 nm for 20 min to detect the absorption of the reaction product of 2,6-DMP. Measurements at the Ultrospec device where done with 2 s intervals and a bandwidth of 2 nm. Measurements at the Tecan device where done with a bandwidth of 9 nm and a settle time of 150 ms. Each well was red multiple times in a 3×3 pattern with 25 flashes each.

To enable protein purification by immobilized metal ion affinity chromatography (IMAC) the already described protein CgL1 was attached to an N-terminal histidine-tag. The previously cloned plasmid pET-16b_cgl1 gene was used as template DNA.[17] The gene *CgL*1 was amplified by polymerase chain reaction (PCR) with the primer 5′-GGAATTCcatatgGGTCCCTCCCTTCGC-3′ and 5′-CGggatccTCCTTACTCGTAGCGAAGCGAG-3′. Recognition sites for *Nde*I and *BamH*I are underlined. The plasmid containing 10X histidine sequence was used for adding the N-terminal His-tag. The PCR was performed with *Pfu* DNA polymerase under the following conditions: 98 °C for 30 sec, 25 cycles of (98 °C for 10 sec, 66 °C for 20 sec, 72 °C for 45 sec), 72 °C for 5 min. The PCR product was purified, digested with *Nde*I and *Bam*HI and ligated into corresponding sites of the linearized pET-16b vector, resulting in pET-16b_His10-cgl1. The correct insertion was verified by automated DNA sequencing (GATC Biotech, Cologne, Germany).

Expression of CgL1 laccase was performed as previously described.[17] For purification, the supernatant after cell disruption and centrifugation was incubated at 50 °C for 10 min and denatured proteins were removed by centrifugation (48,000×g, 30 min, 4 °C). Immobilized metal affinity chromatography (IMAC) was performed on the ÄKTA purifier 100 (GE Healthcare Life Science, Freiburg, Germany) and monitored at 290 nm and 600 nm. The protein sample was applied on a 2×5 ml HisTrap FF Crude column (GE Healthcare Life Science), pre-equilibrated with 50 mM potassium phosphate buffer + 500 mM NaCl, pH 7.5. Proteins were eluted from the column stepwise. Proteins bound with low affinity were washed out by two washing steps (10 mM imidazole and 40 mM imidazole). The target protein was eluted with 125 mM imidazole. Fractions containing laccase activity (measured with 2,2′-azino-bis(3-ethylbenzothiazoline-6-sulphonic acid as substrate (so called ABTS assay, see below)) were pooled and concentrated by ultrafiltration (membrane cut-off 10 kDa).

The protein solution was incubated with 2 mM $CuSO_4$ for 2 h and desalted by gel filtration using a PD MidiTrap G-25 column (GE Healthcare Life Science). Total protein concentrations were determined using the Bradford assay and bovine serum albumin as standard.

Following a modified procedure reported in reference [54] 2-methylimidazole (2.874 g, 35 mmol) and $Zn(NO_3)_2 \cdot 6H_2O$ (149 mg, 0.5 mmol) were dissolved in 10 mL and 1 mL of purified water, respectively, and mixed together while stirring. After 5 minutes, the solvent was removed and the solid residue was washed two times with purified H_2O. The product was dried overnight at 100 °C and resulted in a yield of 73 ± 12 mg (52% based on zinc nitrate). For sorption measurements the composite was activated for 24 h at 120 °C in vacuum and analyzed as described in the analytical methods section. Analysis was done by PXRD (Figure 1), AAS (Table S1), N_2-sorption (Figure 4), Ar-sorption (Figure S1) and SEM (Figure 2).

For laccase@ZIF-8 preparation, a portion of 0.25 mL of laccase (15 mg/mL) in 50 mM potassium phosphate buffer, pH 7.5, was added to a solution of 2.874 g (35 mmol) 2-methylimidazole in 10 mL of purified water. Then 149 mg (0.5 mmol) zinc nitrate hexahydrate in 1 mL of purified water were added to the mixture

© 2019 The Authors. Published by Wiley-VCH Verlag GmbH & Co. KGaA

and stirred for 5 minutes at 500 rpm. The resulting suspension was centrifuged for 10 minutes at 10000 rpm and the solid residue was washed two times with 10 mL of purified water. The resulting solid composite was dried overnight at 40 °C and gave a reproducible yield of 100 ± 10 mg. For sorption measurements the composite was activated for 24 h at 120 °C in vacuum and analyzed as described in the analytical methods section. Analysis was done by PXRD (Figure 1), AAS (Table S1), N_2-sorption (Figure 4), Ar-sorption (Figure S1) and SEM (Figure 2).

To determine the copper concentration in laccase@ZIF-8, 103 ± 6 mg of the composite was dissolved in 1 mL of concentrated (37%) hydrochloric acid and diluted with purified water to a total volume of 20 mL. For comparison and reference, a dissolved sample from neat ZIF-8 was prepared the same way as the composite. Also, 250 μL of a 15 mg/mL laccase solution was diluted in purified water to a total of 20 mL volume. The solutions were then analyzed with atomic absorption spectroscopy to determine the copper concentration and subsequently the mass% Cu relative to mass laccase, composite or ZIF-8 (Table S1).

Enzyme activity was determined in 2 mL volume in a 12-multiwell-plate reader (Tecan infinite M200 PRO) at room temperature if not stated otherwise. Reactions were performed in 50 mM potassium phosphate buffer, pH 7.5, with 5 mM 2,6-dimethoxyphenol (2,6-DMP) and 15 mg laccase@ZIF-8 or 2μL of 15 mg/mL free laccase. The increase of absorbance resulting from 2,6-DMP oxidation was monitored at 468 nm ($\varepsilon = 49{,}600\ M^{-1}\ cm^{-1}$). Measurements were done using a bandwidth of 9 nm at a settle time of 150 ms. Each well was read multiple times in a 3×3 pattern with 25 flashes each. One unit of activity (U) is defined as the amount of enzyme/composite that converts 1 μmol 2,6-DMP per minute.

For laccase stability determination, 15 mg of laccase@ZIF-8 were added to 50 mM potassium phosphate buffer, pH 7.5 (2000 μL), containing 5 mM 2,6-DMP. The increase of absorbance was monitored at 468 nm in a well on a 12-multiwell-plate.

To determine solvent stability of encapsulated laccase, 15 mg of laccase@ZIF-8 were suspended in 1 mL of a chosen solvent (DMF, ethanol) and incubated for 1 h at room temperature. The solvent was removed by centrifugation at 30000 rpm for 5 min. The activity of the residue was determined as described above.

For thermal stability, multiple samples of 15 mg of laccase@ZIF-8 were suspended in 1 mL of potassium phosphate buffer (50 mM, pH 7.5). The samples were incubated at different temperatures (room temperature, 40, 60, 70 °C) for 1 h, 4 h and 6 h. Afterwards the enzyme activity was determined as described above. The large error bars in Figure 6 are an artefact from the increase in absorption due to the movement of the TECAN-multiwell reader during the measurement. Due to a lack of better procedures, the measurements were done with a method not completely optimized for dispersions. The activity was measured with a dispersion, in which the particles were kept in motion during the measurement only by the movement of the multiwell plate in the Tecan reader (see Figure S2 and S3 in Supp. Info.). Yet, this movement caused larger MOF particles to move into the beam, causing a decrease of transmission, that is, an artefact-increase in absorption. These artefacts did only occur in the temperature stability tests, causing the very large error bars at some points. All measurements were done from at least two independent experiments with three replicates each.

To evaluate leaching of laccase from the laccase@ZIF-8 composite, the reaction with 2,6-DMP was carried out as described in the previous section. Activity measurements were stopped after 8 minutes, the solid was removed by centrifugation at 30000 rpm for 15 min. 2,6-DMP was again added to the remaining solution and absorbance change was followed at 468 nm.

For substrate specificity, multiple samples of laccase@ZIF-8 were prepared depending on the used substrate. For 2,6-DMP and syringaldazine, the composite was suspended in 1800 μL potassium phosphate buffer, pH 7.5, and 200 μL of 50 mM 2,6-DMP or syringaldazine were added. The increase of absorbance was monitored at 468 and 525 nm, respectively. For ABTS the composite was suspended in 1800 μL sodium acetate buffer. pH 5.0, and 200 μL of 50 mM ABTS. The increase of absorbance was monitored at 405 nm.

Additionally, atomic absorption spectroscopy was carried out with the reaction solution and the solid residue. Both samples where dissolved in 1 mL of concentrated HCl and diluted with purified water to a total volume of 20 mL.

Conflict of Interest

The authors declare no conflict of interest.

Keywords: laccase · metal-organic frameworks · ZIF-8 · enzyme encapsulation · enzyme stabilization · substrate specificity

[1] H. Griengl, H. Schwab, M. Fechter, *Trends Biotechnol.* **2000**, *18*, 252–256.
[2] L. Martínková, V. Křen, *Biocatal. Biotransform.* **2009**, *20*, 73–93.
[3] J. F. Kennedy, H. Kumar, P. S. Panesar, S. S. Marwaha, R. Goyal, A. Parmar, S. Kaur, *J. Chem. Technol. Biotechnol.* **2006**, *81*, 866–876.
[4] U. T. Bornscheuer, *Angew. Chem. Int. Ed.* **2003**, *42*, 3336–3337.
[5] S. F. M. van Dongen, J. A. A. W. Elemans, A. E. Rowan, R. J. M. Nolte, *Angew. Chem. Int. Ed. Engl.* **2014**, *53*, 11420–11428.
[6] M. Hartmann, D. Jung, *J. Mater. Chem.* **2010**, *20*, 844–857.
[7] K. Liang, C. J. Coghlan, S. G. Bell, C. Doonan, P. Falcaro, *Chem. Commun.* **2016**, *52*, 473–476.
[8] Y. Chen, S. Han, X. Li, Z. Zhang, S. Ma, *Inorg. Chem.* **2014**, *53*, 10006–10008.
[9] X. Wu, M. Hou, J. Ge, *Catal. Sci. Technol.* **2015**, *5*, 5077–5085.
[10] J. Mehta, N. Bhardwaj, S. K. Bhardwaj, K.-H. Kim, A. Deep, *Coord. Chem. Rev.* **2016**, *322*, 30–40.
[11] S. Pang, Y. Wu, X. Zhang, B. Li, J. Ouyang, M. Ding, *Process Biochem.* **2016**, *51*, 229–239.
[12] J. Huo, J. Aguilera-Sigalat, S. El-Hankari, D. Bradshaw, *Chem. Sci.* **2015**, *6*, 1938–1943.
[13] Y. Chen, V. Lykourinou, T. Hoang, L.-J. Ming, S. Ma, *Inorg. Chem.* **2012**, *51*, 9156–9158.
[14] F.-K. Shieh, S.-C. Wang, C.-I. Yen, C.-C. Wu, S. Dutta, L.-Y. Chou, J. V. Morabito, P. Hu, M.-H. Hsu, K. C.-W. Wu, *JACS* **2015**, *137*, 4276–4279.
[15] W. Chen, W. Yang, Y. Lu, W. Zhu, X. Chen, *Anal. Methods* **2017**, *9*, 3213–3220.
[16] A. U. Czaja, N. Trukhan, U. Muller, *Chem. Soc. Rev.* **2009**, *38*, 1284–1293.
[17] E. Ricklefs, N. Winkler, K. Koschorreck, V. B. Urlacher, *J. Biotechnol.* **2014**, *191*, 46–53.
[18] R. Reiss, J. Ihssen, L. Thöny-Meyer, *BMC Biotechnol.* **2011**, *11*, 9.
[19] Z. Zhang, X. Zhang, B. Liu, J. Liu, *JACS* **2017**, *139*, 5412–5419.
[20] J. S. Chen, Y. S. Dagdas, B. P. Kleinstiver, M. M. Welch, A. A. Sousa, L. B. Harrington, S. H. Sternberg, J. K. Joung, A. Yildiz, J. A. Doudna, *Nature* **2017**, *550*, 407–410.
[21] J. M. Bolivar, L. Wilson, S. A. Ferrarotti, J. M. Guisán, R. Fernández-Lafuente, C. Mateo, *J. Biotechnol.* **2006**, *125*, 85–94.
[22] G. Irazoqui, C. Giacomini, F. Batista-Viera, B. M. Brena, *J. Mol. Catal. B* **2007**, *46*, 43–51.
[23] U. Hanefeld, L. Gardossi, E. Magner, *Chem. Soc. Rev.* **2009**, *38*, 453–468.
[24] K. Liang, R. Ricco, C. M. Doherty, M. J. Styles, S. Bell, N. Kirby, S. Mudie, D. Haylock, A. J. Hill, C. J. Doonan, P. Falcaro, *Nat. Commun.* **2015**, *6*, 7240–7247.
[25] X. Wu, J. Ge, C. Yang, M. Hou, Z. Liu, *Chem. Commun.* **2015**, *51*, 13408–13411.

© 2019 The Authors. Published by Wiley-VCH Verlag GmbH & Co. KGaA

[26] F. Lyu, Y. Zhang, R. N. Zare, J. Ge, Z. Liu, *Nano Lett.* **2014**, *14*, 5761–5765.
[27] P. Baldrian, *FEMS Microbiol. Rev.* **2006**, *30*, 215–242.
[28] H. Claus, *Micron* **2004**, *35*, 93–96.
[29] E. I. Solomon, P. Chen, M. Metz, S.-K. Lee, A. E. Palmer, *Angew. Chem. Int. Ed.* **2001**, *40*, 4570–4590; *Angew. Chem.* **2001**, *113*, 4702–4724.
[30] A. M. Mayer, R. C. Staples, *Phytochem. Lett.* **2002**, *60*, 551–565.
[31] L. Munk, A. K. Sitarz, D. C. Kalyani, J. D. Mikkelsen, A. S. Meyer, *Biotechnol. Adv.* **2015**, *33*, 13–24.
[32] U. N. Dwivedi, P. Singh, V. P. Pandey, A. Kumar, *J. Mol. Catal. B: Enzym.* **2011**, *68*, 117–128.
[33] S. Rodriguez Couto, J. L. Toca Herrera, *Biotechnol. Adv.* **2006**, *24*, 500–513.
[34] J.-M. Bollag, A. Leonowicz, *Appl. Environ. Microbiol.* **1984**, *48*, 849–854.
[35] V. Madhavi, S. S. Lele, *BioResources* **2009**, *4*, 1694–1717.
[36] S. Ba, A. Arsenault, T. Hassani, J. P. Jones, H. Cabana, *Crit. Rev. Biotechnol.* **2013**, *33*, 404–418.
[37] M. Fernández-Fernández, M. Á. Sanromán, D. Moldes, *Biotechnol. Adv.* **2013**, *31*, 1808–1825.
[38] V. Gascón, E. Castro-Miguel, M. Díaz-García, R. M. Blanco, M. Sanchez-Sanchez, *J. Chem. Technol. Biotechnol.* **2017**, *92*, 2583–2593.
[39] V. Gascón, M. B. Jiménez, R. M. Blanco, M. Sanchez-Sanchez, *Catal. Today* **2018**, *304*, 119–126.
[40] S. Pang, Y. Wu, X. Zhang, B. Li, J. Ouyang, M. Ding, *Process Biochem.* **2016**, *51*, 229–239.
[41] S. Patra, S. Sene, C. Mousty, C. Serre, A. Chaussé, L. Legrand, N. Steunou, *ACS Appl. Mater. Interfaces* **2016**, *8*, 20012–20022.
[42] P. D. Patil, G. D. Yadav, *ChemistrySelect* **2018**, *3*, 4669–4675.
[43] M. Naseri, F. Pitzalis, C. Carucci, L. Medda, L. Fotouhi, E. Magner, A. Salis, *ChemCatChem* **2018**, *10*, 5425–5433.
[44] K. S. Park, Z. Ni, A. P. Cote, J. Y. Choi, R. Huang, F. J. Uribe-Romo, H. K. Chae, M. O'Keeffe, O. M. Yaghi, *PNAS* **2006**, *103*, 10186–10191.
[45] Y. Pan, Y. Liu, G. Zeng, L. Zhao, Z. Lai, *Chem. Commun.* **2011**, *47*, 2071–2073.
[46] S. B. Novaković, G. A. Bogdanović, C. Heering, G. Makhloufi, D. Francuski, C. Janiak, *Inorg. Chem.* **2015**, *54*, 2660–2670.
[47] J. Cravillon, S. Münzer, S.-J. Lohmeier, A. Feldhoff, K. Huber, M. Wiebcke, *Chem. Mater.* **2009**, *21*, 1410–1412.
[48] Y. Pan, D. Heryadi, F. Zhou, L. Zhao, G. Lestari, H. Su, Z. Lai, *CrystEngComm* **2011**, *13*, 6937–6940.
[49] N. L. Torad, M. Hu, Y. Kamachi, K. Takai, M. Imura, M. Naito, Y. Yamauchi, *Chem. Commun.* **2013**, *49*, 2521–2523.
[50] X.-C. Huang, Y.-Y. Lin, J.-P. Zhang, X.-M. Chen, *Angew. Chem. Int. Ed.* **2006**, *45*, 1587–1589.
[51] C.-W. Tsai, E. H. Langner, *Microporous Mesoporous Mater.* **2016**, *221*, 8–13.
[52] K. Liang, R. Ricco, C. M. Doherty, M. J. Styles, S. Bell, N. Kirby, S. Mudie, D. Haylock, A. J. Hill, C. J. Doonan, *Nat. Commun.* **2015**, *6*, 7240–7247.
[53] F. Lyu, Y. Zhang, R. N. Zare, J. Ge, Z. Liu, *Nano Lett.* **2014**, *14*, 5761–5765.
[54] Y. Pan, Y. Liu, G. Zeng, L. Zhao, Z. Lai, *Chem. Commun.* **2011**, *47*, 2071–2073.

Manuscript received: April 26, 2019
Revised manuscript received: June 29, 2019

© 2019 The Authors. Published by Wiley-VCH Verlag GmbH & Co. KGaA